RAA 2018 Vol. **18** No. **9**, 109(6pp) doi: 10.1088/1674–4527/18/9/109

http://www.raa-journal.org *http://iopscience.iop.org/raa*

***R**esearch in*
***A**stronomy and*
***A**strophysics*

Searching for γ-ray counterparts to very faint X-ray transient neutron star binaries

Ge-Ge Wang[1,2] and Zhong-Xiang Wang[1]

[1] Shanghai Astronomical Observatory, Chinese Academy of Sciences, Shanghai 200030, China; *wangzx@shao.ac.cn*

[2] University of Chinese Academy of Sciences, Beijing 100049, China

Received 2018 January 15; accepted 2018 April 26

Abstract Very faint X-ray transients (VFXTs) are a group of X-ray binaries with low luminosities, displaying peak X-ray luminosities during their outbursts of only 10^{34}–10^{36} erg s^{-1}. Using γ-ray data obtained with the Large Area Telescope (LAT) onboard the *Fermi Gamma-Ray Space Telescope* (*Fermi*), we investigate their possible nature of containing rotation-powered pulsars, or more specifically being transitional millisecond pulsars (MSPs). Among more than 40 known VFXTs, we select 12 neutron star systems. We analyze the LAT data for the fields of 12 VFXTs in the energy range 0.2–300 GeV, but do not find any counterparts likely detected by *Fermi*. We obtain luminosity upper limits for the 12 sources. While the distances to the sources are largely uncertain, the upper limits are comparable to the luminosities of two transitional systems, PSR J1023−0038 and XSS J12270−4859. From our study, we conclude that no evidence is found at γ-rays for the suggestion that some VFXTs could contain rotation-powered MSPs (or be transitional MSP systems).

Key words: stars: pulsars — stars: binaries — gamma rays: stars

1 INTRODUCTION

The discovery of a millisecond pulsar (MSP) in the low-mass X-ray binary (LMXB) SAX J1808.4−3658 (Wijnands & van der Klis 1998) has provided long-sought evidence for the evolution scenario that MSPs form from neutron star LMXBs (Alpar et al. 1982; Radhakrishnan & Srinivasan 1982). The multi-wavelength properties of this so-called accretion-powered MSP system actually suggest that in its quiescent state when its X-ray luminosity is $\sim 5\times10^{31}$ erg s^{-1}, the neutron star switches to be a rotation-powered pulsar (Burderi et al. 2003; see also Wang et al. 2013 and references therein). A similar feature has also been suggested to occur in other accretion-powered MSP systems (e.g., D'Avanzo et al. 2007, 2009). The subsequent discovery of transitional MSP binary PSR J1023+0038 (Archibald et al. 2009) has helped make the picture clearer. This system has shown that it can switch between the states of being a normal radio pulsar binary and having an accretion disk around the neutron star (e.g., Archibald et al. 2009; Wang et al. 2009; Stappers et al. 2014; Takata et al. 2014). More recently, the neutron star binaries J1824−2452I (Papitto et al. 2013) and XSS J12270−4859 (Bassa et al. 2014; de Martino et al. 2014), where the first is located in the globular cluster M28, have also been found to be able to switch between these states. The transitional pulsar binaries show again that at the end of LMXB evolution, a system can have both a rotation-powered MSP and an accretion disk.

Based on observational studies of these systems, it can be seen that they share the similar property of having low X-ray luminosities. For example, even in the active state with an accretion disk, PSR J1023+0038 has an X-ray luminosity of only $\sim 6\times10^{33}$ erg s^{-1} (Li et al. 2014). The low luminosity implies a low accretion rate in the disk, and thus the energy output from the neutron star powered by its fast rotation can destroy the weak accre-

tion disk (see, e.g., Wang et al. 2009). X-ray observations of PSR J1023+0038 in its disk-free state have clearly shown the existence of an intrabinary shock region that is the result of interaction between the pulsar wind and outflow of the companion star (Bogdanov et al. 2011). The mass transfer rate must also be low such that outflow from the companion can be stopped from forming an accretion disk by the pulsar wind for years. Following this idea, we may consider that LMXB sources, identified because of their detection in X-ray surveys, may contain rotation-powered pulsars. For example, both PSR J1023+0038 and XSS J12270−4859 in their active state were once considered to be typical LMXBs (Thorstensen & Armstrong 2005; Hill et al. 2011).

The transitional pulsar binaries show again.

Because of low peak X-ray luminosities ($10^{34} - 10^{36}\,\mathrm{erg\,s^{-1}}$) during their outbursts, a group of X-ray binaries is classified as very faint X-ray transients (VFXTs; Wijnands et al. 2006). While their nature of being so faint is poorly understood (e.g., Heinke et al. 2015), observations in the past 10 years have established that a fraction of VFXTs is neutron star LMXBs, due to the detection of thermonuclear type I X-ray bursts (see, e.g., Campana 2009). It has thus been pointed out that some of these neutron star binary systems could correspond to the active state of transitional MSP systems (Heinke et al. 2015). Given that both PSR J1023+0038 and XSS J12270−4859 have shown significant γ-ray emission during their active states (actually their γ-ray fluxes were several times brighter than those in their disk-free state), γ-ray observations of VFXTs can be used to explore this possibility.

The *Fermi Gamma-Ray Space Telescope* (*Fermi*), which was launched in June of 2008, has the Large Area Telescope (LAT) onboard. The unprecedented sensitivity of the LAT at γ-rays has allowed us to study both Galactic and extragalactic high-energy sources in detail. Thus far, more than 3000 sources have been detected by the LAT (Acero et al. 2015). In this paper, we report our search for the γ-ray counterparts to 12 neutron star VFXTs (see Table 1) from the analysis of LAT all-sky survey data. These VFXTs were selected from more than 40 identified VFXTs, a list of which is summarized in Liu & Li (2017). In our selection, we avoided the Galactic center and globular cluster sources; the extremely high source density in these regions does not allow a clear identification of any faint sources in the *Fermi* data.

2 *Fermi* LAT DATA ANALYSIS AND RESULTS

2.1 *Fermi* LAT Data

As one of the two instruments onboard *Fermi*, LAT is an imaging γ-ray telescope scanning the whole sky every three hours in the energy range from 20 MeV to 300 GeV (Atwood et al. 2009). In the analysis reported in this paper, the LAT data for each target were selected from the latest *Fermi* Pass 8 database within 20° of the target's position. The observing time period of the data was from 2008 August 4 15:43:39 to 2016 November 1 00:00:00 (UTC), nearly 8.25 years. To avoid relatively large uncertainties in the instrument response function of LAT in the low energy range, the energy range we used was from 200 MeV to 300 GeV. In addition, following the recommendations of the LAT team[1], we selected events with zenith angles less than 90° to exclude possible contamination from Earth's limb.

2.2 Maximum Likelihood Analysis

Using the newly released LAT science tools package `v10r0p5`, we conducted standard binned maximum likelihood analysis (Mattox et al. 1996) on the data for each target. The source model of a target contained all the sources, based on the LAT 4-year catalog (Acero et al. 2015), within 20° centered at the target's position. The normalization parameters and spectral indices of the sources within 5° from each target were set as free parameters and all the other parameters were fixed at their catalog values in the LAT catalog. We included Galactic and extragalactic diffuse emission by using the model gll_iem_v06.fits and spectrum file iso_P8R2_SOURCE_V6_v06.txt in the source model, respectively. The normalization parameters of the two diffuse emission components were set as free parameters. For each of the 12 VFXT targets, we applied a simple power law as the source model.

We calculated test statistic (TS) maps of a $3^\circ \times 3^\circ$ region centered at the position of each target. TS values are derived from $\mathrm{TS} = -2\log(L_0/L_1)$, where L_0 and L_1 are the maximum likelihood values for a model having none or an additional source at a given position respectively (Abdo et al. 2010). The TS value for a detected source is approximately equal to the square of the detection significance (Abdo et al. 2010).

[1] *http://fermi.gsfc.nasa.gov/ssc/data/analysis/scitools/*

Table 1 Luminosity Upper Limits in 0.2–300 GeV for the 12 VFXTs

Source Name	R.A. (h m s)	Dec. (° ′ ″)	Distance (kpc)	$L_\gamma/10^{35}$ (erg s^{-1})	Type
SAX J1324.5−6313	13:24:27.00	–63:13:24.00	<6.2	0.2	Burst-only
SAX J1753.5−2349	17:53:31.90	–23:49:14.86	<8.8	0.09	Burst-only
SAX J1752.3−3138	17:52:24.00	–31:37:42.00	<9.2	0.7	Burst-only
SAX J1806.5−2215	18:06:32.18	–22:14:17.20	<8.0	0.04	Burst-only
SAX J1818.7+1424	18:18:44.00	+14:24:12.00	<9.4	0.04	Burst-only
SAX J1828.5−1037	18:28:33.00	–10:37:48.00	<6.2	0.7	Burst-only
SAX J2224.9+5421	22:24:52.00	+54:21:54.00	<7.1	0.03	Burst-only
1RXS J170854.4−321857	17:08:52.50	–32:19:26.00	13±2.0	0.09	Persistent
RX J1718.4−4029	17:18:24.13	–40:29:30.40	<6.5 or <9.0	0.3	Persistent
RX J1735.3−3540	17:35:23.75	–35:40:16.00	<6.2 or <9.5	0.5	Persistent
AX J1754.2−2754	17:54:14.47	–27:54:36.10	<6.6 or <9.2	0.04	Persistent
Swift J185003.2−005627	18:50:03.33	–00:56:23.30	<3.7	0.3	Others

In the TS maps we obtained, an extended region with high TS values was detected around the target SAX J1828.5−1037 (see the left panel of Figure 1). For all other targets, no such regions or possible point-like sources with sufficiently high TS values were seen. We further analyzed the data for SAX J1828.5−1037 by calculating a 1–300 GeV TS map. In this higher energy range, the spatial resolution of LAT is significantly improved to be approximately 1° (68% containment angle; see details in the LAT performance note[2]). The TS map is shown in the right panel of Figure 1, and it can be seen that there is no γ-ray source at the source's position and the high TS values at low energy ranges are likely caused by the pulsar J1828−1101 to the south of SAX J1828.5−1037.

2.3 Variability Search

All these targets are variable sources in the X-ray band. For example, X-ray outbursts were reported in SAX J1753.5−2349 (Del Santo et al. 2010), SAX J1806.5−2215 (Altamirano et al. 2011) and Swift J185003.2−005627 (Degenaar et al. 2012) after *Fermi* was launched. We therefore searched for detections considering if they had significant variations during the *Fermi* LAT coverage. For each target, we divided the whole 8.25 years of data into bins with two time durations, 30 d and 180 d, and performed likelihood analysis on the data in each time bin. However, the TS values at the position of each target did not show any possible detections. We concluded that no target was detected in the time bins of either 30 d or 180 d.

[2] *http://www.slac.stanford.edu/exp/glast/groups/canda/lat_Performance.htm*

2.4 Luminosity Upper Limit Estimation

We estimated the γ-ray flux upper limits of the 12 VFXTs, performing binned likelihood analysis with the source models described above. The spectral normalization factors were set as free parameters. Following the procedure given by the LAT team, we obtained the 95% flux upper limits in the 0.2–300 GeV energy range by increasing the flux values until the maximum likelihood values decreased by $e/2$ in logarithm. In the calculations, the photon index Γ of the power law was set the same as that of the transitional MSP binary PSR J1023+0038 in its disk-free state, which is 2.4. While the distances to the VFXTs are highly uncertain, most of them have upper limits, estimated by setting the burst peak luminosities equal to the Eddington limit (e.g., Campana 2009).

In Table 1, the distance values summarized by Liu & Li (2017) are given. Using these values, we obtained the upper limits on the γ-ray luminosities, which are provided in Table 1. Note that because of different assumptions for the bursts, three sources have two different distance upper limits. We always used the larger values.

3 DISCUSSION

Having selected 12 neutron star systems from more than 40 known VFXTs, we have investigated their possible nature at γ-ray energies. The data were from the *Fermi* LAT all-sky survey at the energy range of 0.2–300 GeV. The motivation was that if some neutron star VFXTs are the type of X-ray binaries similar to accretion-powered MSP or transitional MSP binaries, we would expect possible detection of them at γ-rays since they could switch to be rotation powered in quiescence or have bright γ-ray emission such as in the active state of the transitional

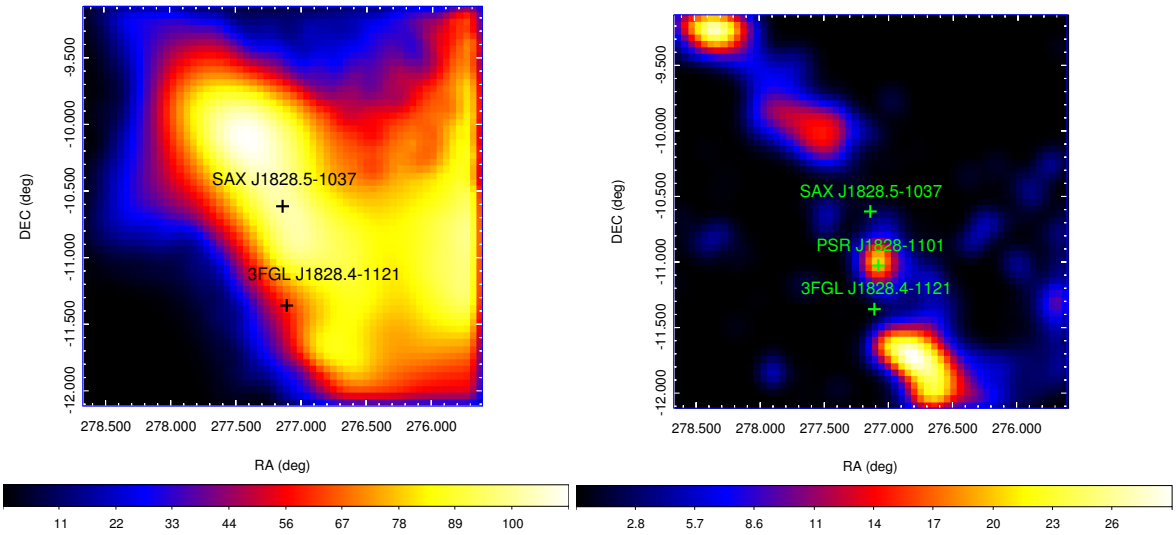

Fig. 1 TS maps for SAX J1828.5−1037 in the energy range of 0.2–300 GeV (*left panel*) and 1–300 GeV (*right panel*). The image scale is 0.05° pixel^{-1}. The positions of the LAT third source catalog (3FGL) J1828.4−1121, PSR J1828−1101 and SAX J1828.5−1037 are marked with *crosses*.

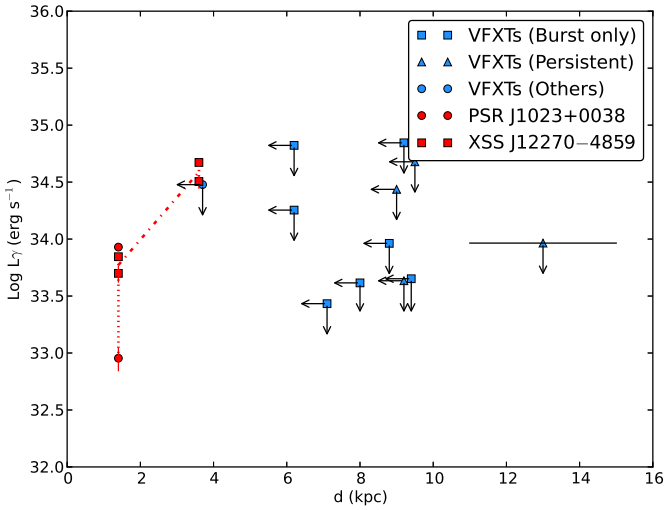

Fig. 2 Luminosity upper limits in 0.2–300 GeV for the 12 VFXTs. Also shown are the luminosity ranges of the transitional MSP binaries PSR J1023+0038 (*red circles*) and XSS J12270−4859 (*red squares*) between the active and disk-free states. Because XSS J12270−4859 is known with a distance range of 1.4–3.6 kpc, we show both luminosity ranges at 1.4 and 3.6 kpc.

MSP binaries. However from our analysis of 8.25-year LAT data, we did not detect any possible candidates. We note that nearly all of these sources, except SAX J1818.7+1424, are located in the Galactic disk (Galactic latitudes smaller than 5°) and most of them are close to the direction of the Galactic center (due to the designed X-ray monitoring; e.g., Wijnands et al. 2006). Our search was hampered by the crowdedness in the fields. There are often several bright sources in a source field of $3° \times 3°$ we considered (such as in Fig. 1), and they made a clear search for any faint sources difficult.

Using the estimated upper limits on the γ-ray luminosities of the VFXTs in 0.2–300 GeV, we can compare them with the two transitional MSP binaries PSR J1023+0038 and XSS J12270−4859, whose γ-ray emission was relatively well studied by *Fermi* LAT.

In Figure 2, we show the upper limits for the VFXTs and the luminosity ranges of the two transitional MSP

binaries. Note that for most VFXTs, their distances only have upper limits. Since in the active state of the latter two sources, their γ-ray luminosities were significantly brighter (Stappers et al. 2014; Xing & Wang 2015), we plotted both luminosities in the disk-free and active states. In addition, the distance to XSS J12270−4859 is rather uncertain (e.g., Roy et al. 2015; Rivera Sandoval et al. 2018), and we considered the range of 1.4–3.6 kpc. The comparison shows that the upper limits of the VFXTs are actually comparable to the luminosity ranges of the two transitional MSPs. For XSS J12270−4859, in the disk-free state even assuming the low distance value of 1.4 kpc, a few of the VFXTs' upper limits are already lower than its luminosity. For PSR J1023+0038, its disk-free luminosity was $\simeq 10^{33}\,\mathrm{erg\,s^{-1}}$ (Tam et al. 2010), and the upper limits have not reached such a low level.

Among the 12 VFXTs, seven are classified as burst-only sources (Table 1; see also Liu & Li 2017), which implies that they had extremely low persistent X-ray emission (X-ray luminosities lower than $10^{33}\,\mathrm{erg\,s^{-1}}$). There are four persistent sources, which are defined because they have X-ray luminosities at the level of $\sim 10^{34}\,\mathrm{erg\,s^{-1}}$. In order to explain temporal properties of VFXTs' X-ray emission, Heinke et al. (2015) suggested that persistent VFXTs could be transitional MSPs in the active state. In Figure 2, we can see that one of the persistent sources has an upper limit lower than the active-state luminosities of both transitional MSPs. In addition, three burst-only sources have upper limits below the luminosity of XSS J12270−4859 in its disk-free state (during which radio pulsed emission has been detected; Roy et al. 2015). From the comparison, we may conclude that no evidence is found at γ-rays to support VFXTs contain pulsars. However, we should be cautious that pulsars have a large range of γ-ray luminosity values due to different properties of the pulsars or geometric effects (Abdo et al. 2013), and even for the active state of transitional MSPs, how their enhanced γ-ray emission is produced is still not clear (Papitto & Torres 2015).

Acknowledgements This research made use of the High Performance Computing Resource in the Core Facility for Advanced Research Computing at Shanghai Astronomical Observatory. This research was supported by the National Program on Key Research and Development Project (Grant No. 2016YFA0400804) and the National Natural Science Foundation of China (11633007). Z.W. acknowledges support by the CAS/SAFEA International Partnership Program for Creative Research Teams.

References

Abdo, A. A., Ackermann, M., Ajello, M., et al. 2010, ApJS, 188, 405
Abdo, A. A., Ajello, M., Allafort, A., et al. 2013, ApJS, 208, 17
Acero, F., Ackermann, M., Ajello, M., et al. 2015, ApJS, 218, 23
Alpar, M. A., Cheng, A. F., Ruderman, M. A., & Shaham, J. 1982, Nature, 300, 728
Altamirano, D., Kaur, R., Degenaar, N., et al. 2011, The Astronomer's Telegram, 3193
Archibald, A. M., Stairs, I. H., Ransom, S. M., et al. 2009, Science, 324, 1411
Atwood, W. B., Abdo, A. A., Ackermann, M., et al. 2009, ApJ, 697, 1071
Bassa, C. G., Patruno, A., Hessels, J. W. T., et al. 2014, MNRAS, 441, 1825
Bogdanov, S., Archibald, A. M., Hessels, J. W. T., et al. 2011, ApJ, 742, 97
Burderi, L., Di Salvo, T., D'Antona, F., et al. 2003, Chinese Journal of Astronomy and Astrophysics Supplement, 3, 311
Campana, S. 2009, ApJ, 699, 1144
D'Avanzo, P., Campana, S., Casares, J., et al. 2009, A&A, 508, 297
D'Avanzo, P., Campana, S., Covino, S., et al. 2007, A&A, 472, 881
de Martino, D., Casares, J., Mason, E., et al. 2014, MNRAS, 444, 3004
Degenaar, N., Linares, M., Altamirano, D., & Wijnands, R. 2012, ApJ, 759, 8
Del Santo, M., Sidoli, L., Romano, P., et al. 2010, MNRAS, 403, L89
Heinke, C. O., Bahramian, A., Degenaar, N., & Wijnands, R. 2015, MNRAS, 447, 3034
Hill, A. B., Szostek, A., Corbel, S., et al. 2011, MNRAS, 415, 235
Li, K. L., Kong, A. K. H., Takata, J., et al. 2014, ApJ, 797, 111
Liu, B. S., & Li, X. D. 2017, Progress in Astronomy, 35, 190 (in Chinese)
Mattox, J. R., Bertsch, D. L., Chiang, J., et al. 1996, ApJ, 461, 396
Papitto, A., & Torres, D. F. 2015, ApJ, 807, 33
Papitto, A., Ferrigno, C., Bozzo, E., et al. 2013, Nature, 501, 517
Radhakrishnan, V., & Srinivasan, G. 1982, Current Science, 51, 1096
Rivera Sandoval, L. E., Hernández Santisteban, J. V., Degenaar, N., et al. 2018, MNRAS, 476, 1086

Roy, J., Ray, P. S., Bhattacharyya, B., et al. 2015, ApJ, 800, L12
Stappers, B. W., Archibald, A. M., Hessels, J. W. T., et al. 2014, ApJ, 790, 39
Takata, J., Li, K. L., Leung, G. C. K., et al. 2014, ApJ, 785, 131
Tam, P. H. T., Hui, C. Y., Huang, R. H. H., et al. 2010, ApJ, 724, L207
Thorstensen, J. R., & Armstrong, E. 2005, AJ, 130, 759
Wang, Z., Archibald, A. M., Thorstensen, J. R., et al. 2009, ApJ, 703, 2017
Wang, Z., Breton, R. P., Heinke, C. O., Deloye, C. J., & Zhong, J. 2013, ApJ, 765, 151
Wijnands, R., & van der Klis, M. 1998, Nature, 394, 344
Wijnands, R., in't Zand, J. J. M., Rupen, M., et al. 2006, A&A, 449, 1117
Xing, Y., & Wang, Z. 2015, ApJ, 808, 17